Determination of the electron diffusion length in dye sensitized solar cells by substrate contact patterning.

Halina K. Dunn[1‡], Per-Oskar Westin[2], Daniel R. Staff[3], Laurence M. Peter[4], Alison B. Walker[3], Gerrit Boschloo[1] and Anders Hagfeldt[1].*

1. Institute of Physical and Analytical Chemistry, Uppsala University, box 259, 751 05 Uppsala, Sweden

2. Solid state electronics, Uppsala University, Box 534, 751 21 Uppsala, Sweden

3. Department of Physics, University of Bath, Bath BA2 7AY, UK

4. Department of Chemistry, University of Bath, Bath BA2 7AY, UK

Received Date:

e-mail: halina.dunn@fki.uu.se

‡ Current address: Departament de Física, Universitat Jaume I, 12071 Castelló de la Plana, Spain

ABSTRACT

A new method to estimate the electron diffusion length in dye-sensitized solar cells (DSCs) is presented. DSCs were fabricated on conducting glass substrates that were patterned by laser ablation of the FTO coating to form parallel contact strips separated by uncontacted strips of the same width. The relative collection efficiency was measured as a function of the gap between the contact strips, which determines the lateral distance traveled by electrons to reach the contacts. In order to avoid complications arising from non-linear recombination kinetics, current measurements were performed using small amplitude perturbations of the electron density close to open circuit and the maximum power point to minimize electron density gradients in the film. One and two dimensional solutions of the continuity equation for electron transport and back reaction predict that the relative collection efficiency should fall as spacing between the contact strips exceeds the electron diffusion length and electrons are lost by back electron transfer during transit to the contacts. Measurements of the relative collection efficiency were fitted to the predicted dependence of collection efficiency on the spacing between the contact strips to obtain the value of the electron diffusion length. The diffusion length is found to increase with voltage both at open circuit and at the maximum power point.

KEYWORDS: dye-sensitized solar cell, diffusion length, patterned substrate

Introduction

Since the original work of Grätzel and O'Regan[1], dye sensitized solar cells (DSC) have been studied intensively. The basic concepts of their operation have been reviewed in detail elsewhere.[2] Briefly, a wide bandgap porous semiconductor, typically TiO_2, is sensitised with a dye which absorbs visible light. The photoexcited dye injects electrons into the TiO_2 conduction band and is regenerated subsequently by electron transfer from iodide ions in the electrolyte permeating the porous structure. The injected electrons travel to the back contract, where they are extracted and re-enter the cell via a platinized counter electrode, to reduce the I_3^- ions formed in the regeneration step. Ionic diffusion between the electrodes completes the cycle.

The electron diffusion length, L_0, which is the average distance an electron can diffuse in the TiO_2 before recombining with tri-iodide ions (assuming negligible recombination with oxidized dye species). If recombination TiO_2 electrons with tri-iodide occurs via 1st order kinetics, then the diffusion length can be defined as;

$$L_0 = \sqrt{\tau_0 D_0} \tag{1}$$

where τ_0 is the free electron lifetime, and D_0 is the free electron diffusion coefficient. For efficient collection of electrons in a DSC, the electron diffusion length needs to be at least 2-3 times larger than the thickness of the TiO_2 film. The electron diffusion length can be obtained by dynamic methods, such as impedance spectroscopy[3] or the analysis of the response time of the photovoltage and photocurrent to small perturbations in light intensity[4-6], and by steady state methods, such as the comparison of the incident photon to electron conversion efficiency (IPCE)

spectra from front and rear side illumination.[7-9] Several comparisons of these different techniques have been made, and in some cases diffusion lengths determined by steady state methods are shorter than those determined by dynamic methods.[10,11] Recently, it has been suggested that the rate of recombination of electrons in the TiO_2 with tri-iodide in the electrolyte is not first order in free electron concentration, meaning that the diffusion length can only be defined for a given electron concentration.[12] A local electron density-dependent diffusion length, λ_n, is thus defined according to:

$$\lambda_n = \left(\frac{D_0 n_b^{1-\beta}}{\beta k_r} \right)^{1/2} \quad (2)$$

where n_b is the background electron concentration, k_r is the rate of back reaction with triiodide, and β is the back reaction order.

The density-dependence of the diffusion length complicates the interpretation of measurements in which the electron concentration is not constant, for example, front/rear side IPCE studies carried out without background illumination.[13] Recently, a very careful comparison has been made between values of the diffusion length obtained by impedance spectroscopy and by front/rear side IPCE measurements using bias light, showing that the methods agree if measurements are made close to open circuit to ensure that the electron concentration across the film is almost constant.[14]

The extraction of the electron diffusion length from IPCE and impedance measurements involves data fitting with a rather large number of parameters. Here, we explore the concept of obtaining the electron diffusion length using a simpler geometrical approach that involves

patterning the substrates into alternating strips of equal width with and without fluorine-doped tin oxide (FTO). The electron collection efficiency is then measured as a function of the separation between the contact strips. One would expect the collection efficiency to fall when the strip separation exceeds the electron diffusion length. Fundamentally, this approach is similar to the front/rear side IPCE method, given that we adjust the distance between the point of generation and the point of collection of carriers. The crucial difference is that this distance is varied in a lateral dimension; thus avoiding the need to account for optical absorption by the electrolyte and platinized cathode, which complicates the analysis of front/rear side IPCE spectra. It also avoids the complications arising from trapping and de-trapping of electrons that influence time and frequency dependent perturbation measurements. More importantly this method can be applied to study cells in which the electron diffusion length is significantly greater than the film thickness so that the IPCE method cannot be used.

Our technique can be used to estimate the electron diffusion length anywhere along the *i-V* curve, in particular close to the maximum power point. Since the measurements are carried out at a steady state, RC time limitations which can be associated with current transient techniques close to open circuit, do not affect our measurements.[15,16]

Modeling

The continuity equation in 2 dimensions was solved using finite element methods to derive the photoinduced conduction band electron concentration profiles $n(x,y)$ in a TiO_2 film (thickness 6.5 microns) contacted by a periodic array of FTO stripes (height taken to be 100 nm) under constant illumination with a photon flux at $y = 0$ of $I_0 = 10^{16}$ cm^{-2} s^{-1}.

$$D_0\nabla^2 c(x,y) + \alpha I_0 e^{-\alpha y} - \frac{n(x,y)}{\tau_0} = 0 \qquad (3)$$

Here α is the optical absorption coefficient of the dyed TiO_2 film at the excitation wavelength (α = 340cm^{-1} at 630 nm) and τ_0 is the free electron lifetime. Figure 1, in which the x and y axes are defined, illustrates the spatial variation of excess electron concentration for the case where the inter-electrode separation, s, is 30 μm and the electron diffusion length is 100 μm. Similar plots in which s is much shorter, similar, and much longer than the diffusion length can be found in the supporting information.

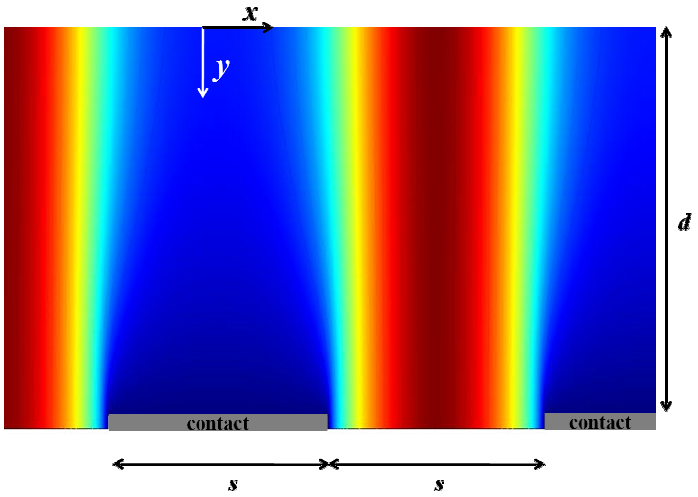

Figure 1: Solution of equation 3 where d=6.5 μm, s = 30μm, L_0=100 μm and τ=1.10^{-4} s, α = 340cm^{-1}, I_0 = 10^{16} cm^{-2} s^{-1}. $n(x,y)$ varies from 0 (dark blue) to 4.85.10^{12} electrons cm^{-3} (dark red). Not to scale.

Provided that the height of the FTO strips is much smaller than the film thickness and the electron diffusion length is larger than the film thickness, the problem reduces to the 1 dimensional case if αd <<1 (weakly absorbed light), so that the electron injection rate is invariant

in the y-direction. In the 1D limit, the concentration of excess electrons in the TiO_2 between the FTO contacts is given by

$$n(x) = \alpha I_0 \tau_0 \left(1 - \frac{e^{x/L_0} + e^{-x/L_0}}{e^{s/2L_0} + e^{-s/2L_0}} \right) \tag{4}$$

where the origin $x = 0$ is taken to be at the center of the gap. If the relative collection efficiency η_{rel} is defined as the flux of electrons leaving the whole device compared to an equivalent device where no FTO has been removed, one can show that

$$\eta_{rel} = \frac{1}{2} + \frac{\tanh(s/2L_0)}{s/L_0} \tag{5}$$

Figure 2 shows that the analytical and numerical solutions for η_{rel} are in close agreement when L_0=100 μm is much greater that the film thickness (6.5 μm). We note that in these calculations, we have assumed a unity back reaction order. Therefore fits to equation 5 are only valid if the measurements are carried out under conditions in which there is a steady background electron concentration.

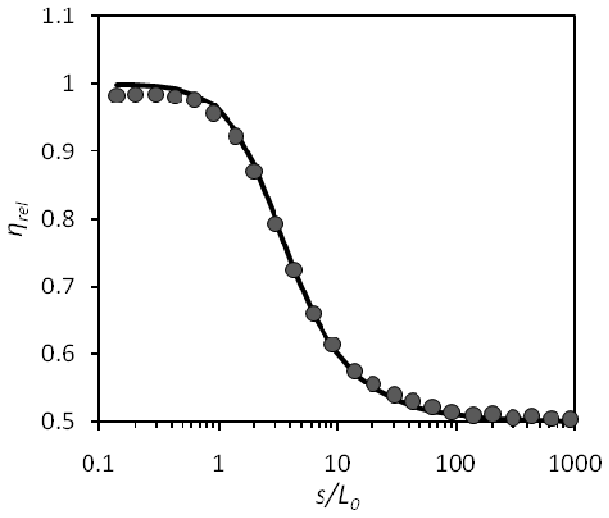

Figure 2: Modeled relative collection efficiency as a function of s/L_0 calculated based on solutions to the continuity equation in one (solid line) and two dimensions (circles).

Experimental

Solar cell preparation on patterned substrates

After cleaning the FTO glass (TEC 15 Pilkington TEC Glass™) by sequential sonication in detergent, water and ethanol, a compact blocking layer of TiO_2 was applied by spray pyrolysis of a 0.2 M solution of titanium(IV)-isopropoxide at 500°C. Patterning of substrates was performed using a Nd:YVO_4 diode-pumped solid state laser operating at 532 nm with an XY sample translation stage. The FTO layer was removed by direct induced ablation, with the laser beam incident through the glass substrate. In spite of the low optical absorbance of the FTO layer, removal by laser ablation can be achieved with good results above a certain threshold laser energy density.[17] The compact TiO_2 layer on top of the FTO was also removed in the laser ablated areas. The minimum stripe width was limited by the laser setup to the single laser line width of 33 μm. Adjacent and overlapping laser lines were used to create wider gaps. In all cases the widths of the FTO strips and FTO-free strips were equal, so that 50% of the substrate was

covered with FTO. The strip widths were measured using an Olympus® optical light microscope and Picsara® image analysis software. The laser scribe lines were checked to ensure that they were indeed electrically isolated and had a near square profile (Figure 3).

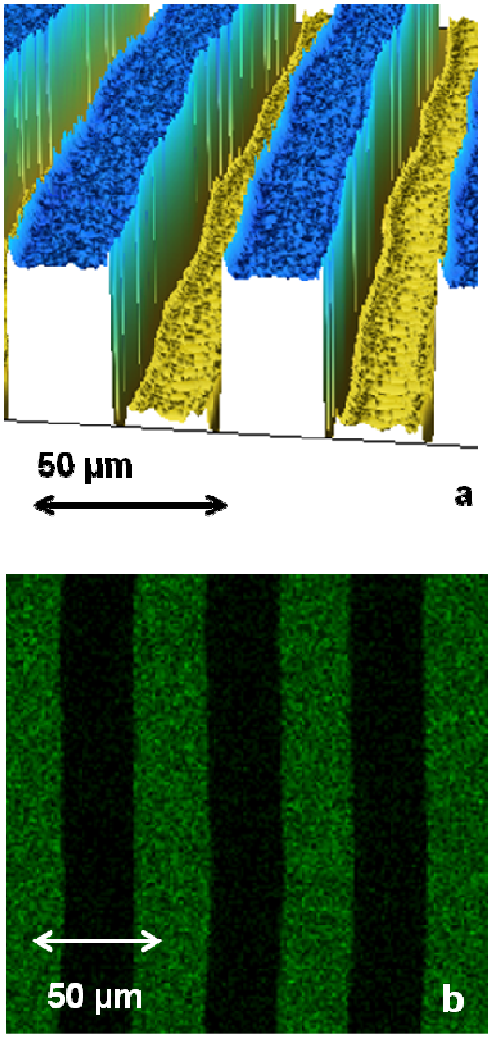

Figure 3: (a) White light interferometry image of the patterned appearance. Laser scribing clears patches between strips of FTO. During patterning the strip widths were varied while maintaining a 50% FTO coverage. (b) SEM-EDS image showing the Sn signal from the FTO layer.

Substrates of 8 different strip/gap widths (33, 50, 80, 120, 170, 250, 500 and 1000 μm) were prepared. On average 5 solar cells were built with each substrate type, as well as controls with full FTO coverage. A 6 by 8 mm porous TiO_2 layer was deposited on the substrates by screen printing (Dyesol DSL 18NR-T) and heated to 500°C for 30 minutes to remove the organic components. After sensitization of the TiO_2 films in a 0.5 mM solution of N719 (Dyesol) in acetonitrile:tert-butanol overnight, the cells were sealed using a 50 μm Surlyn spacer. Electrolyte (0.5 M LiI, 0.06M I_2, 0.6M propyl methyl imidazolium iodide, 0.1M guanidinium thiocyanide, 0.5M tert-butyl pyridine in 3-methoxypropionitrile) was introduced via pre-drilled holes in the platinized counter electrode, which was prepared by thermal decomposition of a 5 mM solution H_2PtCl_6 at 390°C for 30 min. The film thicknesses (which range from 5.5 to 8 μm) were determined using a Veeco Dektak 3 profilometer. All solvents and reagents were purchased from Sigma Aldrich, unless otherwise stated.

Small amplitude current measurements.

Cells were illuminated through the front contact by a power LED (Thorlabs, 627 nm), the intensity of which was controlled by the use of neutral density filters (Thorlabs). Cells were connected to an Autolab potentiostat (AUTOLAB Pgstat 10) operating in 2 electrode mode, and the current-voltage (*i-V*) characteristics were recorded. To make comparisons between cells at different points along the *i-V* curve, we defined the applied potential, V_{app}, in terms of the current flowing as a fraction of the short circuit current, I_{SC}. Thus, "close to open circuit" was defined as the potential at which $I_{SC}/20$ flows, while "close to the maximum power point" was defined as the potential at which $I_{SC}/1.1$ flows. Once these bias voltages were determined, the light intensity was stepped up and down by 5% of the dc value. A 5s up/down cycle was chosen to ensure that steady state current values were recorded. The small current increments, *dI*, caused by the pulse

were recorded using the Autolab potentiostat in chronoamperometric mode. Figure 4 shows some example current voltage curves for cells built on ordinary and patterned substrates, as well as the applied potential "close to open circuit" (indicated by circular markers) and "close to the maximum power point" (diamond markers).

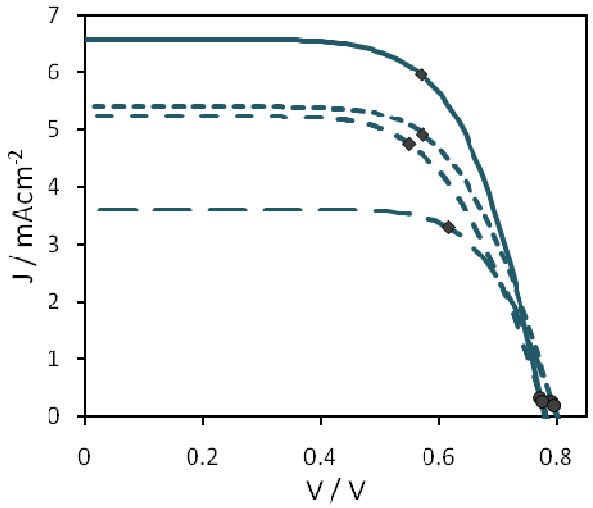

Figure 4: *i-V* curves for and ordinary cell (full line) and cells with 30, 120 and 250 µm patterning (represented by the smallest to largest dashed lines, respectively). The circular markers indicate the potential applied to work close to open circuit, while the diamonds indicate the maximum power point. Illumination at 627nm, photon flux: 10^{17} $cm^{-2}s^{-1}$.

Results and discussion

Relative collection efficiency as a function of strip width at open circuit

By carrying out measurements using small amplitude light perturbations close to open circuit or close to the maximum power point under weakly absorbed illumination, complications arising from the density dependence of the diffusion length when there is a non-uniform electron concentrations were avoided. Since αd <1, the current measurements are sensitive to variations

in film thickness (see supporting information). For this reason, a correction was made to allow for variations in film thickness between different cells. The thickness dependence of the small amplitude current delivered by the ordinary cells was quantified (see supporting information) and used to calculate η_{rel} for individual patterned cells based on the current expected from an ordinary cell of the same film thickness, δI_{pred}.

$$\eta_{rel} = \frac{\delta I}{\delta I_{pred}(d)} \tag{6}$$

The relative collection efficiency of electrons generated over the areas without FTO can be seen in Figure 5 under open circuit conditions under an illumination intensity of $9x10^{16}$ $cm^{-2}s^{-1}$. There is a plateau up to finger separations of 80 μm, after which the collection drops off rapidly. This implies that the diffusion length is of the order of 80 μm in this case. In order to obtain a more accurate value for the diffusion length, the data are fit to equation 5 with the diffusion length as the only free parameter. Contrary to the theoretical prediction, the plateau in the experimental η_{rel} values is less than 100%, 85% in this case. Therefore the data have been normalised to the first data point to allow comparison to the results of equation 5. The origin of this discrepancy is not clear at present, although we tentatively suggest that reduced scattering of light as a consequence of removing the FTO layer may lower the extent to which photons are harvested by the cell.

Each data point corresponds to an average of 5-7 cells (except the point corresponding to 1000 μm, which is reflected by the larger error bars). The error of the mean was therefore calculated as the individual error divided by the square root of the number of samples. We take the

individual error as the spread in plots of δI *vs* d of the 8 ordinary cells (see supporting information). In most cases, this error was 10-15 %, except close to open circuit at the highest light intensity. A strong correlation of the small amplitude currents with film thickness implies that the light harvesting efficiency is the main variable determining the IPCE, with the collection and injection efficiencies appearing to be constant. The 10% scatter in the data can be attributed to slight variations between samples, and imperfections in the film thickness determination. Koops *et al.* have found there to be a slight decrease in the injection efficiency under applied potential, particularly as the potential reaches the open circuit voltage under one sun illumination.[18] As the Fermi level increases, it reaches a critical energy at which the injection efficiency begins to decrease. If this critical energy were slightly different for the different samples, this could explain the larger scatter in δI for the highest light intensity under open circuit conditions

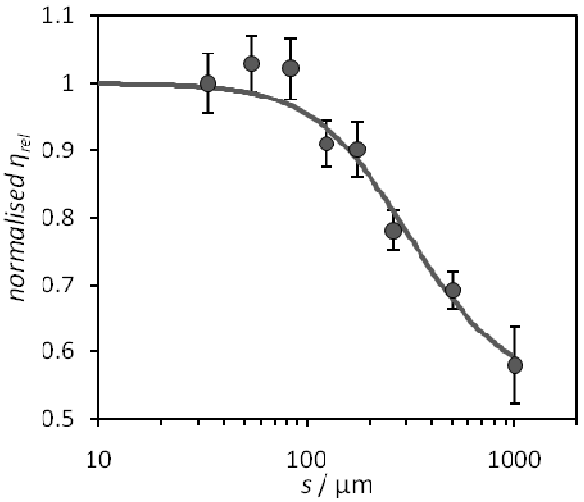

Figure 5: Normalized relative collection efficiency as a function of stripe width close to open circuit under 627nm illumination of intensity $9x10^{15}cm^{-2}s^{-1}$. Data normalized to the first data point: 85%. The line is a fit of equation 5 with L_0=90µm.

Relative collection efficiency as a function of strip width at the maximum power point

As mentioned previously, there is a large uncertainty in η_{rel} under open circuit conditions at the highest light intensity, which induces a similar current as under one sun illumination. However, a good fit was obtained close to the maximum power point, which is, in fact, the most useful for practical reasons. Although current is being extracted at the maximum power point, the electron concentration in the film remains almost constant (see the solution to equation 3 in the supporting information). For this reason, the electron diffusion length defined by equation 2 is valid at the maximum power point, similarly to under open circuit conditions.

Figure 6 shows that the normalized η_{rel} at the maximum power point also exhibits a plateau at shorter stripe widths, after which it decreases rapidly. The best fit to equation 5 yields a diffusion length of 82 μm.

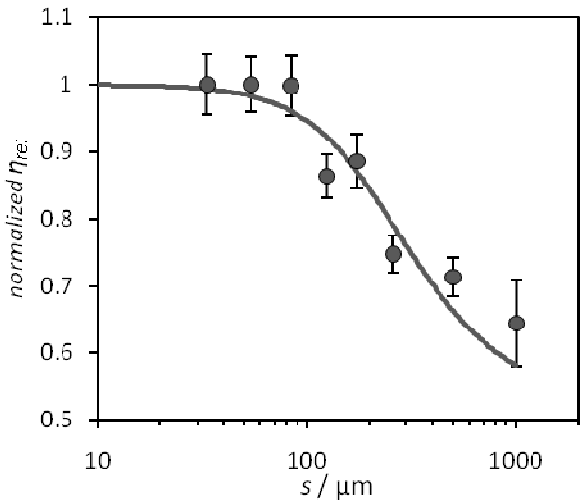

Figure 6: Relative collection efficiency as a function of stripe width determined close to the maximum power point under illumination (627 nm 10^{17} $cm^{-2}s^{-1}$) which leads to a cell short circuit current density similar to that at one Sun. Data normalized to the first data point: 75%. The line is a fit of equation 5 with L_0=82µm.

Diffusion length as a function of Fermi Level position

The diffusion length estimations at open circuit and at the maximum power point have been compiled in Figure 7. As predicted by equation 2, if $\beta < 1$, the diffusion length, of the order of 100µm, increases with voltage (and therefore electron concentration). These observations are in agreement with diffusion length studies employing a range of different techniques, including impedance spectroscopy, comparison of front and rear side illumination and frequency resolved small amplitude perturbation techniques. [3,9,10,13,14]

We also note that the data points acquired at the maximum power point (light grey markers) lie slightly shifted to lower voltages than the open circuit values (dark grey markers). This is expected since the diffusion length at the maximum power point is defined by the overall electron density across the thickness of the film, which is inherently slightly higher than the electron

density, and hence voltage, at the contact, since charges are extracted under these conditions – see supporting information.

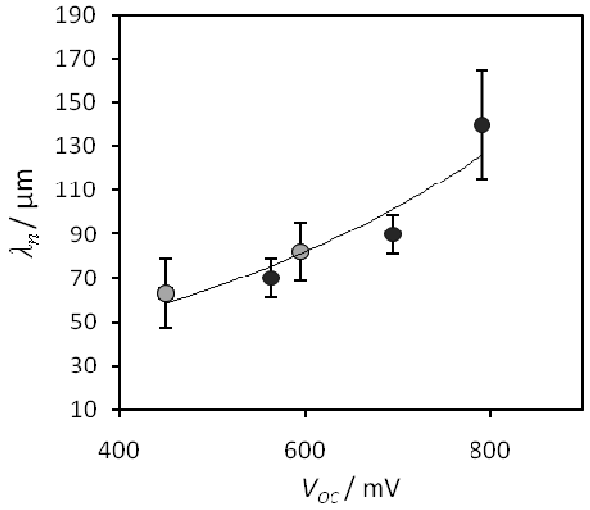

Figure 7: Diffusion length values determined from the relative collection efficiency under 627 nm illumination at open circuit (black circles) and close to the maximum power point (gray circles). The fit corresponds to a back reaction order, β, of 0.88.

Conclusions

The method presented herein offers a simple and intuitive determination of the diffusion length in DSCs. By constructing solar cells on substrates with patterned electron collectors of different widths, we are able to directly assess how far charges are able to travel before recombination with tri-iodide occurs. We are also able to determine the diffusion length at the maximum power point. The diffusion length, of the order of 100 µm, is found to increase with quasi Fermi level, as is expected if the reaction order for the reaction of TiO_2 electrons with tri-iodide is less than one, as is widely reported in the literature.

The patterned cells developed in this work could have interesting applications in other subfields of DSC research. By opening up a variable in a second dimension, namely parallel to the substrate, the method could lend itself very well to the study of devices in which the film thickness is empirically limited, but without a full understanding of the causes. For example, the optimum thickness of devices employing solid hole-transport materials are often much smaller than for those containing liquid electrolytes. However, diffusion length studies which use the film thickness as a variable introduce variations in secondary parameters, such as reduced pore-filling, or limited hole-transport in the hole-conducting material. For example, the optimum film thickness for cells employing spiro-OMeTAD is approximately 2-3 μm, even though small amplitude measurements (with an additional internal contact to monitor the electron concentration under short circuit conditions) suggest that the electron diffusion length is much larger.[19] Furthermore, these results could be relevant to research in alternative cell design, for example in the fabrication of tandem geometries employing a mesh-like internal electrode[20].

Supporting information available:

Solutions of the 2D model (as in Figure 1) for various electrode separations. IPCE and optical absorption data, further details of error analysis and film thickness correction, as well as the other η_{rel} fits used to construct the plot in Figure 7. Calculated electron profiles across the thickness of the film at open circuit, the maximum power point and short circuit.

Acknowledgements:

The authors thank the Wallenberg foundation for funding, and James Jennings, Ute Cappel and Martin Karlsson for interesting discussions.

References:

(1) Oregan, B.; Gratzel, M. *Nature* **1991**, *353*, 737.

(2) Peter, L. M. *Journal of Physical Chemistry C* **2007**, *111*, 6601.

(3) Bisquert, J.; Fabregat-Santiago, F.; Mora-Sero, I.; Garcia-Belmonte, G.; Gimenez, S. *Journal of Physical Chemistry C* **2009**, *113*, 17278.

(4) Peter, L. M.; Ponomarev, E. A.; Fermin, D. J. *Journal of Electroanalytical Chemistry* **1997**, *427*, 79.

(5) Dunn, H. K.; Peter, L. M. *Journal of Physical Chemistry C* **2009**, *113*, 4726.

(6) Peter, L. M.; Wijayantha, K. G. U. *Electrochemistry Communications* **1999**, *1*, 576.

(7) Sodergren, S.; Hagfeldt, A.; Olsson, J.; Lindquist, S. E. *Journal of Physical Chemistry* **1994**, *98*, 5552.

(8) Halme, J.; Boschloo, G.; Hagfeldt, A.; Lund, P. *Journal of Physical Chemistry C* **2008**, *112*, 5623.

(9) Barnes, P. R. F.; Anderson, A. Y.; Koops, S. E.; Durrant, J. R.; O'Regan, B. C. *Journal of Physical Chemistry C* **2009**, *113*, 1126.

(10) Wang, H. X.; Peter, L. A. *Journal of Physical Chemistry C* **2009**, *113*, 18125.

(11) Barnes, P. R. F.; Liu, L. X.; Li, X. E.; Anderson, A. Y.; Kisserwan, H.; Ghaddar, T. H.; Durrant, J. R.; O'Regan, B. C. *Nano Letters* **2009**, *9*, 3532.

(12) Bisquert, J.; Mora-Sero, I. *Journal of Physical Chemistry Letters*, *1*, 450.

(13) Villanueva-Cab, J.; Wang, H. X.; Oskam, G.; Peter, L. M. *Journal of Physical Chemistry Letters*, *1*, 748.

(14) Jennings, J. R.; Li, F.; Wang, Q. *Journal of Physical Chemistry C*, *114*, 14665.

(15) Nissfolk, J.; Fredin, K.; Hagfeldt, A.; Boschloo, G. *Journal of Physical Chemistry B* **2006**, *110*, 17715.

(16) O'Regan, B. C.; Bakker, K.; Kroeze, J.; Smit, H.; Sommeling, P.; Durrant, J. R. *Journal of Physical Chemistry B* **2006**, *110*, 17155.

(17) Compaan, A. D.; Matulionis, I.; Nakade, S. *Optics and Lasers in Engineering* **2000**, *34*, 15.

(18) Koops, S. E.; O'Regan, B. C.; Barnes, P. R. F.; Durrant, J. R. *Journal of the American Chemical Society* **2009**, *131*, 4808.

(19) Jennings, J. R.; Peter, L. M. *Journal of Physical Chemistry C* **2007**, *111*, 16100.

(20) Uzaki, K.; Pandey, S. S.; Hayase, S. *Journal of Photochemistry and Photobiology a-Chemistry*, *216*, 104.